SUPPLEMENTAL FIGURE LEGENDS

Supplemental Figure 1. The growth defect of the *Pto* Δ*hopT1-1* strain is specifically rescued in Arabidopsis miRNA-defective mutants.

Five-week-old Col-0 Arabidopsis (WT) plants and indicated genotypes in each panel were dip-inoculated with bacterial strains *Pto* DC3000 (*Pto*) (blue dot), *Pto* Δ*hopT1-1* (green dot) or *Pto* Δ*hopC1* (orange dot) at a concentration of 10^8 cfu/mL. At three days post-inoculation, leaves from three plants were collected and bacterial titers monitored. Each symbol represents a number of bacteria as log (cfu per cm^2) and mean (n=8 or 16) is represented as horizontal line in the dot plots. Independent biological replicates distinct from the one presented in Figure 1 are presented here. **(A)-(B)** Left panel: Growth of wild type *Pto* DC3000 strain (*Pto*) and of *hopT1-1*-deleted bacterial strain (*Pto ΔhopT1-1)* in WT plants and in three different alleles of *ago1* mutants, namely *ago1-25*, *ago1-26* and *ago1-27*. Right panel: Growth of WT *Pto* DC3000 strain (*Pto*) and of *hopC1*-deleted bacterial strain (*Pto ΔhopC1)* in WT plants and in *ago1-27* mutant. **(C)** Growth of WT *Pto* and of *Pto ΔhopT1-1* in WT plants and in mutants defective in AGO2 (*ago2-1*) or in AGO4 (*ago4-2* and *ago4-3*). **(D)-(E)** Same as in (A-Left panel) but in miRNA biogenesis-defective mutants: *se-1* and *dcl1-11*. **(F)-(G)** Same as in (C) but in siRNA biogenesis-defective mutants: *sgs3-1, rdr1-1 rdr2-1 rdr6-15*, *dcl2-1 dcl4-2*. Statistical significance for all the above experiments was assessed using the ANOVA test (*: p-value < 0.05; **: p-value < 0.01; ***: p-value < 0.001; ****: p-value < 0.0001).

Supplemental Figure 2. Protein accumulation level of HopT1-1 and of HopT1-1m3 transiently expressed in *N. benthamiana* leaves

(A) *Agrobacterium tumefaciens* strains carrying *Myc-HopT1-1* or *Myc-HopT1-1m3* constructs were infiltrated in four-week-old *N. benthamiana* leaves. Non-infiltrated *N. benthamiana* leaves were used as a control. Protein accumulation level of HopT1-1 and of HopT1-1m3 was monitored at 3 dpi by immunoblotting. An arrow indicates the band corresponding specifically to HopT1-1 and HopT1-1m3 detected using anti-Myc antibody. Relative quantification was performed using anti-hsc70 antibody. Both proteins exhibit stable accumulation *in planta*. **(B)** To perform FRET-FLIM analysis, four-week-old *N. benthamiana* leaves were infiltrated with CFP-AGO1 alone or with YFP-tagged HopT1-1 or HopT1-1m3. After 2 dpi, protein accumulation level was monitored by immunoblotting using anti-GFP antibody. Ponceau staining was used to show equal protein loading for each sample. **(C)** Same as (B), but using CFP-AGO1 alone or with HopT1-1-HA using anti-HA antibody. **NB:** FRET occurs when the fluorescence of an acceptor molecule increases because of non-radiative transfer of energy from a donor molecule to the acceptor. However, quantitative interpretation of intensity-based images is sometimes difficult because of the number of factors that may contribute to intensity variations. For example, fluorophore intensity is related to both its local concentration and quantum yield (Gryczynski, Z. & Lakowicz, J.R. in Molecular Imaging 21–56 Academic Press, 2005). To overcome such difficulties, FLIM (fluorescence lifetime imaging) has been developed as a complementary approach. Since lifetime is known to be related only to the fluorescence quantum yield and not to the fluorescence intensity, lifetime measurements are not influenced by the accumulation level of the fluorescent fusion proteins. Therefore, the lower expression of HopT1-1m3 compared to HopT1-1 reported in this supplemental figure

has no influence on our FRET/FLIM data showing that HopT1-1, but not HopT1-1m3, physically interacts with AGO1.

Supplemental Figure 3. Accumulation level of streptavidin-associated peptides containing each GW and GF motif of HopT1-1 and HopT1-1m3, respectively

To perform the pull-down experiment, we first assessed the accumulation level of streptavidin-associated peptides containing each GW and GF motif of HopT1-1 and HopT1-1m3 respectively, by using dot blot assay. The biotinylated peptides were immobilized with HRP-streptavidin beads and then were spotted on a nitrocellulose membrane at three different amounts (1 µg, 0.1 µg and 0.01 µg). The presence of peptides was revealed by adding ECL substrate.

Supplemental Figure 4. HopT1-1 suppresses AGO1-mediated miRNA function in a GW-dependent manner

(A) The expression of HopT1-1 was monitored by RT-qPCR analysis in individual primary transformants expressing HopT1-1 or HopT1-1m3 under the constitutive 35S promoter. Number of individuals analysed in each condition is n=12. *Actin* was used as a control. **(B)** Expression of endogenous miRNA targets was monitored by RT-qPCR analysis in the same HopT1-1 transgenic plants as well as in individual WT and *ago1-27* mutant plants. The miRNA that targets the analyzed transcript is indicated between brackets. *Actin* was used as a control. **(C)** Relative mRNA accumulation levels of RNA silencing factors targeted by miRNAs were monitored by RT-qPCR analysis in the same plants described in (B). AGO4 was used as an internal control, as this silencing factor is not targeted by any miRNA. *Actin* was used as a control. Statistical significance was assessed by comparing the mean (black

bar) of each condition with the mean of WT condition, using one-way ANOVA analysis (*: p-value < 0.05; **: p-value < 0.01; ****: p-value < 0.0001). **(D)** Individuals of the plants depicted in (B) were pooled to monitor by immunoblotting the protein accumulation levels of the RNA silencing factors depicted in (C). PEPC protein accumulation level was used as loading control for each blot. Relative quantification of the protein accumulation using PEPC accumulation level was done using ImageJ software and is indicated below each condition.

Supplemental Figure 5. HopT1-1 triggers a moderate decrease in a subset of conserved Arabidopsis miRNAs, while it does not, or negligibly, interfere with the accumulation of cognate pri-miRNAs

(A) Accumulation levels of endogenous miRNAs in pooled WT plants and in pooled primary transformants expressing HopT1-1 or HopT1-1m3 were assessed by northern blot. U6 was used as a loading control. **(B)** Accumulation levels of endogenous pri-miRNAs were assessed by RT-qPCR in WT plants and in *dcl1-11* and *se-1* mutants (top panels) or in HopT1-1 and HopT1-1m3 transgenic plants (bottom panels). *Ubiquitin5 (ub5)* was used as a control. Statistical significance was assessed by comparing the mean (black bar) of each condition with the mean of WT condition, using one-way ANOVA analysis (*: p-value<0.05; ****: p-value<0.0001).

Supplemental Figure 6. Several effectors encoded by agriculturally important phytopathogens contain canonical GW/WG motifs

Effectors encoded by bacteria (*Xanthomonas campestris*, *Xanthomonas oryzae* and *Xyllela fastidiosa*), oomycetes (*Phytophthora infestans* and *Phytophthora sojae*) or

fungi (*Puccinia graminis* and *Fusarium graminearum*) containing the highest score (matrix AGO-planVir) of GW/WG motifs prediction were retrieved by using the web portal http://www.comgen.pl/whub (Zielezinski A. & Karlowski WM, 2015). A red bar represents each GW or WG motif.

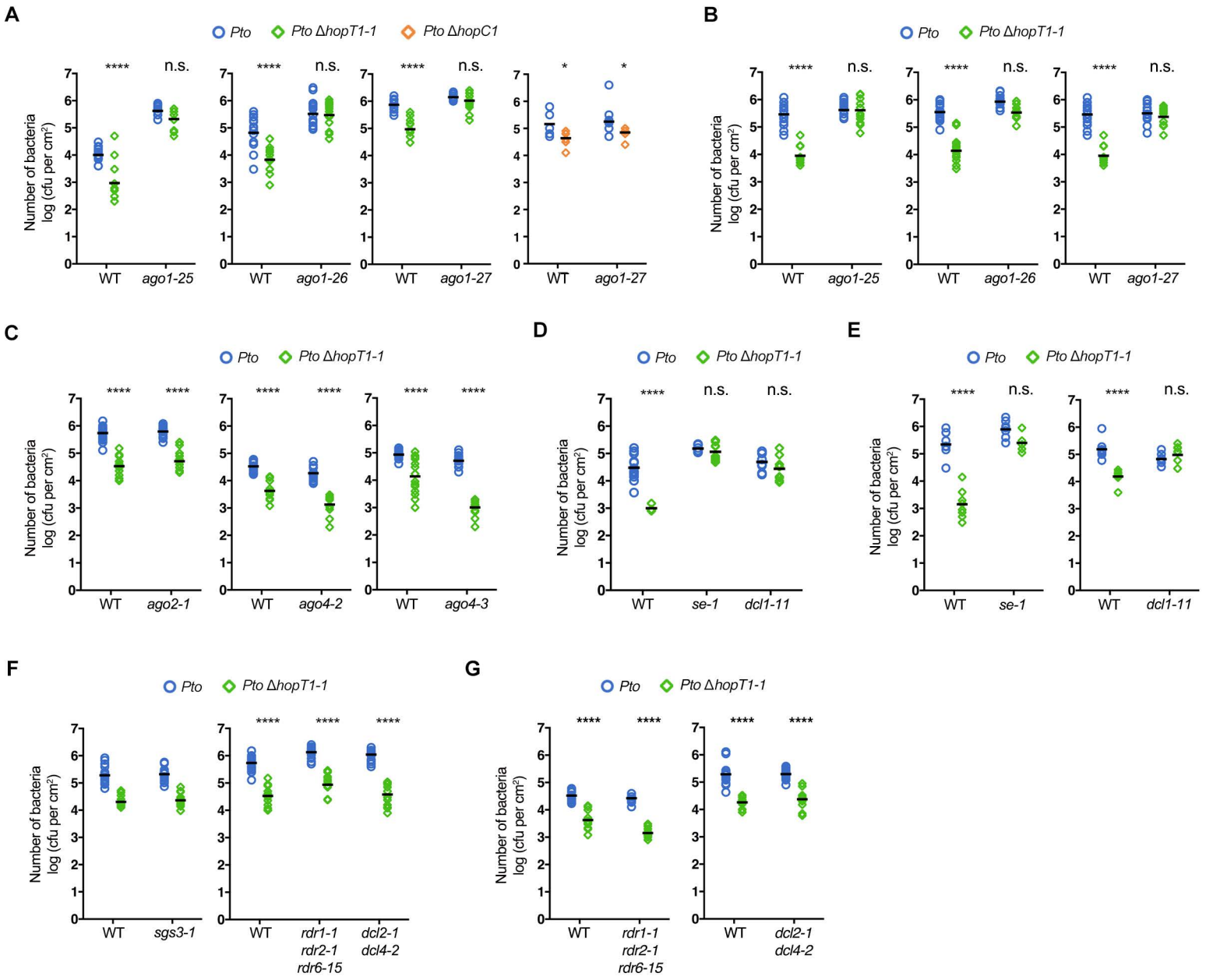

Supplemental Figure 1. The growth defect of the *Pto* ΔhopT1-1 strain is specifically rescued in Arabidopsis miRNA-defective mutants
Five-week-old Col-0 Arabidopsis (WT) plants and indicated genotypes in each panel were dip-inoculated with bacterial strain *Pto* DC3000 (*Pto*) (blue dot), *Pto* ΔhopT1-1 (green dot) or *Pto* ΔhopC1 (orange dot) at a concentration of 10^8 cfu/mL. At three days post-inoculation, leaves from three plants were collected and bacterial titers monitored. Each symbol represents a number of bacteria as log (cfu per cm^2) and mean (n=8 or 16) is represented as horizontal line in the dot plots. Independent biological replicates distinct from one presented in Figure 1 are presented here. **(A)-(B)** Left panel: Growth of WT *Pto* DC3000 strain (*Pto*) and of hopT1-1-deleted bacterial strain (*Pto* ΔhopT1-1) in WT plants and in three different alleles of ago1 mutants, namely *ago1-25*, *ago1-26* and *ago1-27*. Right panel: Growth of wild type *Pto* DC3000 strain (*Pto*) and of hopC1-deleted bacterial strain (*Pto* ΔhopC1) in WT plants and in *ago1-27* mutant. **(C)** Growth of WT *Pto* and of *Pto* ΔhopT1-1 in WT plants and in mutant defective in AGO2 (*ago2-1*) or in AGO4 (*ago4-2* and *ago4-3*). **(D)-(E)** Same as in (A-Left panel) but in miRNA biogenesis-defective mutants: *se-1* and *dcl1-11*. **(F)-(G)** Same as in (C) but in siRNA biogenesis mutants: *sgs3-1*, *rdr1-1 rdr2-1 rdr6-15*, *dcl2-1 dcl4-2*. Statistical significance for all the above experiments was assessed using the ANOVA test (*: p-value < 0.05; **: p-value < 0.01; ***: p-value < 0.001; ****: p-value < 0.0001).

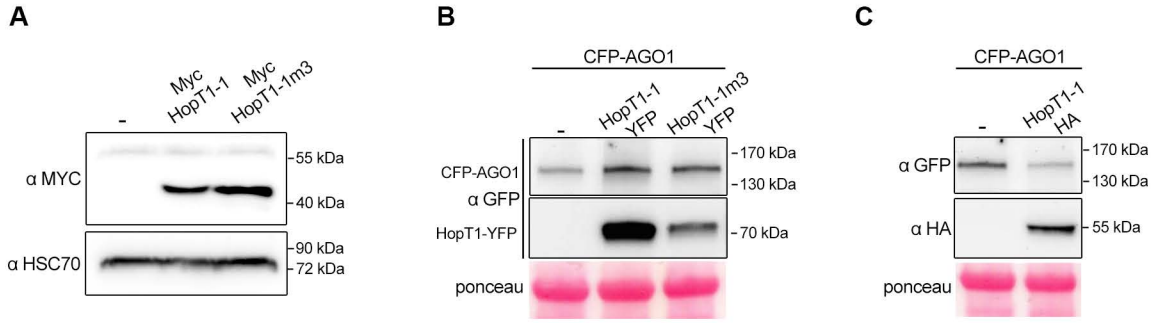

Supplemental Figure 2. Protein accumulation level of HopT1-1 and of HopT1-1m3 transiently expressed in *N. benthamiana* leaves
(A) *Agrobacterium tumefaciens* strains carrying Myc-HopT1-1 or Myc-HopT1-1m3 constructs were infiltrated in four-week-old *N. benthamiana* leaves. Non-infiltrated *N. benthamiana* leaves were used as a control. Protein accumulation level of HopT1-1 and of HopT1-1m3 was monitored at 3 dpi by immunoblotting. Relative quantification was performed using anti-hsc70 antibody. Both the proteins exhibit stable accumulation in planta. **(B)** To perform FRET-FLIM analysis, four-week-old *N. benthamiana* leaves were infiltrated with CFP-AGO1 alone or with YFP-tagged HopT1-1 or HopT1-1m3. After 2 dpi, protein accumulation level was monitored by immunoblotting using anti-GFP antibody. Ponceau staining was used to show equal protein loading for each sample. **(C)** Same as (B), but using CFP-AGO1 alone or with HopT1-1-HA using anti-HA antibody. **NB**: FRET occurs when the fluorescence of an acceptor molecule increases because of non-radiative transfer of energy from a donor molecule to the acceptor. However, quantitative interpretation of intensity-based images is sometimes difficult because of the number of factors that may contribute to intensity variations. For example, fluorophore intensity is related to both its local concentration and quantum yield (Gryczynski, Z., Gryczynski, I. & Lakowicz, J.R. in Molecular Imaging 21–56 Academic Press, 2005). To overcome such difficulties, FLIM (fluorescence lifetime imaging) has been developed as a complementary approach. Since lifetime is known to be related only to the fluorescence quantum yield and not to the fluorescence intensity, lifetime measurements are not influenced by the accumulation level of the fluorescent fusion proteins. Therefore, the lower expression of HopT1-1m3 compared to HopT1-1 reported in this supplemental figure has no influence on our FRET/FLIM data showing that HopT1-1, but not HopT1-1m3, physically interact with AGO1.

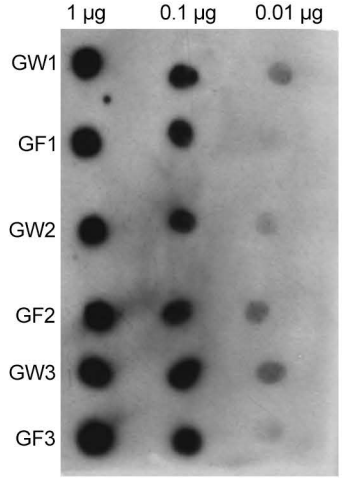

Supplemental Figure 3. Accumulation level of streptavidin-associated peptides containing each GW and GF motif of HopT1-1 and HopT1-1m3, respectively

To perform the pull-down experiment, we first assessed the accumulation level of streptavidin-associated peptides containing each GW and GF motif of HopT1-1 and HopT1-1m3 respectively, by using dot blot assay. The biotinylated peptides were immobilized with HRP-streptavidin beads then were spotted on a nitrocellulose membrane at three different amounts (1 µg, 0.1 µg and 0.01 µg). The presence of peptides was revealed by adding ECL substrate.

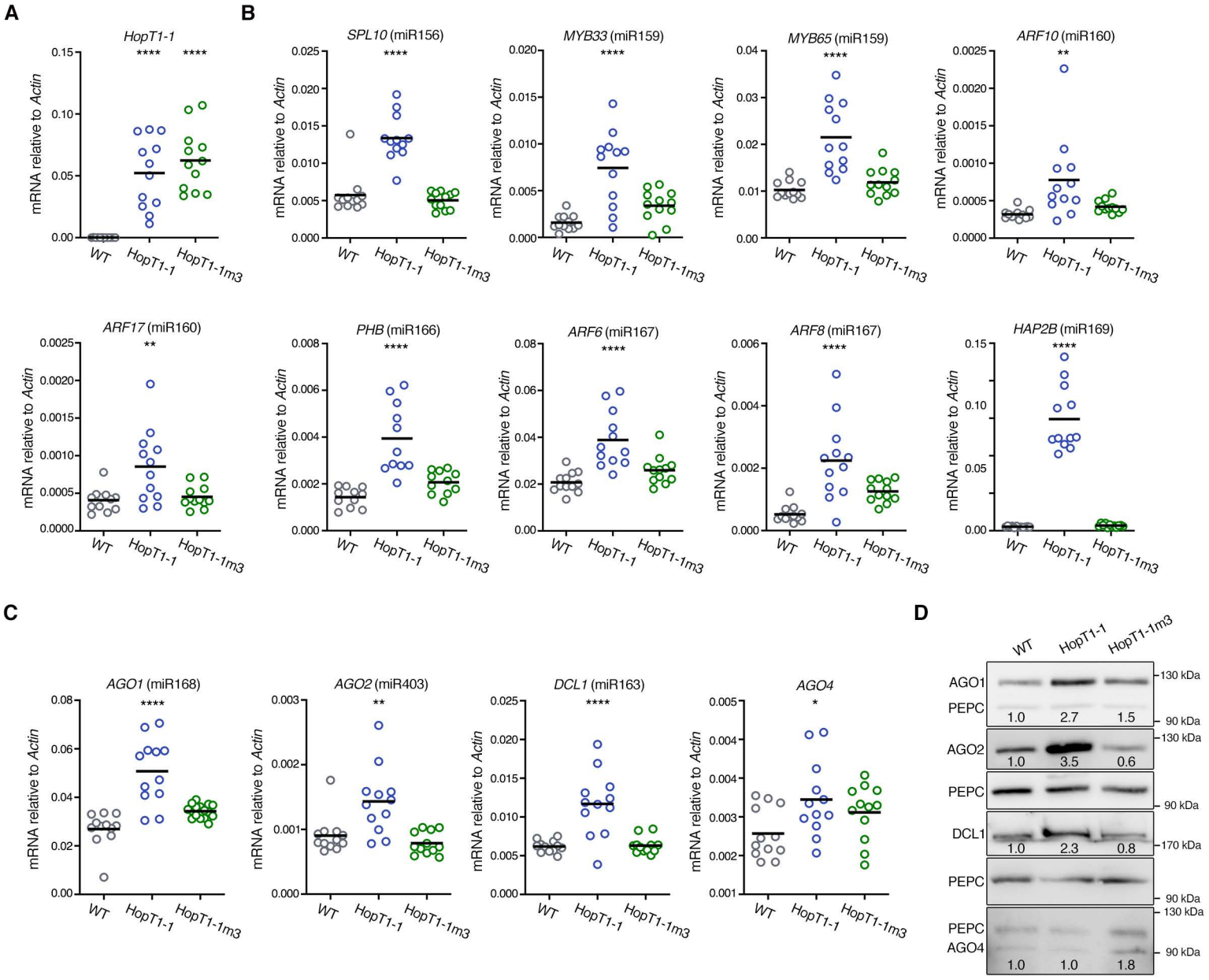

Supplemental Figure 4. HopT1-1 suppresses AGO1-mediated miRNA function in a GW-dependent manner

(A) The expression of HopT1-1 was monitored by RT-qPCR analysis in individual primary transformants expressing HopT1-1 or HopT1-1m3 under the constitutive 35S promoter. Number of individuals analysed in each condition is n=12. Actin was used as a control. **(B)** Expression of endogenous miRNA targets was monitored by RT-qPCR analysis in the same HopT1-1 transgenic plants as well as in individual WT and *ago1-27* mutant plants. The miRNA that targets the analyzed transcript is indicated between brackets. *Actin* was used as a control. **(C)** Relative mRNA accumulation levels of RNA silencing factors targeted by miRNAs were monitored by RT-qPCR analysis in the same plants described in (B). *AGO4* was used as a negative control, as this silencing factor is not targeted by any miRNA. *Actin* was used as a control. **(D)** Individuals of the plants depicted in (B) were pooled to monitor by immunoblotting the protein accumulation levels of the RNA silencing factors depicted in (C). PEPC protein accumulation level was used as loading control for each blot. Relative quantification of the protein accumulation using PEPC accumulation level was done using ImageJ software and is indicated below each condition. For RT-qPCR analyses, statistical significance was assessed by comparing the mean (black bar) of each condition with the mean of WT condition, using one -way ANOVA analysis (*: p-value < 0.05; **: p-value < 0.01; ****: p-value < 0.0001).

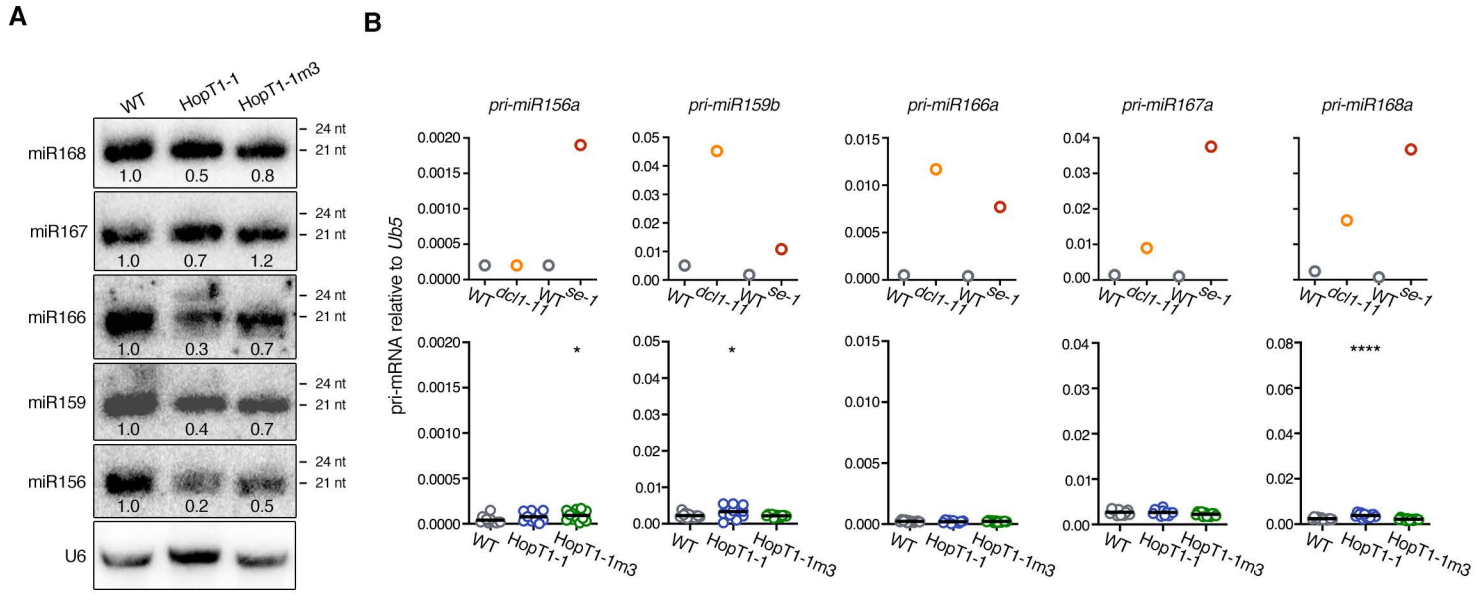

Supplemental Figure 5. HopT1-1 triggers a moderate decrease in a subset of conserved Arabidopsis miRNAs, while it does not, or negligibly, interfere with the accumulation of cognate pri-miRNAs

(A) Accumulation levels of endogenous miRNAs in pooled WT plants and in pooled primary transformants expressing HopT1-1 or HopT1-1m3 were assessed by northern blot. U6 was used as a loading control. **(B)** Accumulation levels of endogenous pri-miRNAs were assessed by RT-qPCR in WT plants and in dcl1-11 and se-1 mutants (top panels) or in HopT1-1 and HopT1-1m3 transgenic plants (bottom panels). *Ubiquitin5* (*ub5*) was used as a control. Statistical significance was assessed by comparing the mean (black bar) of each condition with the mean of WT condition, using one-way ANOVA analysis (*: p-value<0.05; ****: p-value<0.0001).

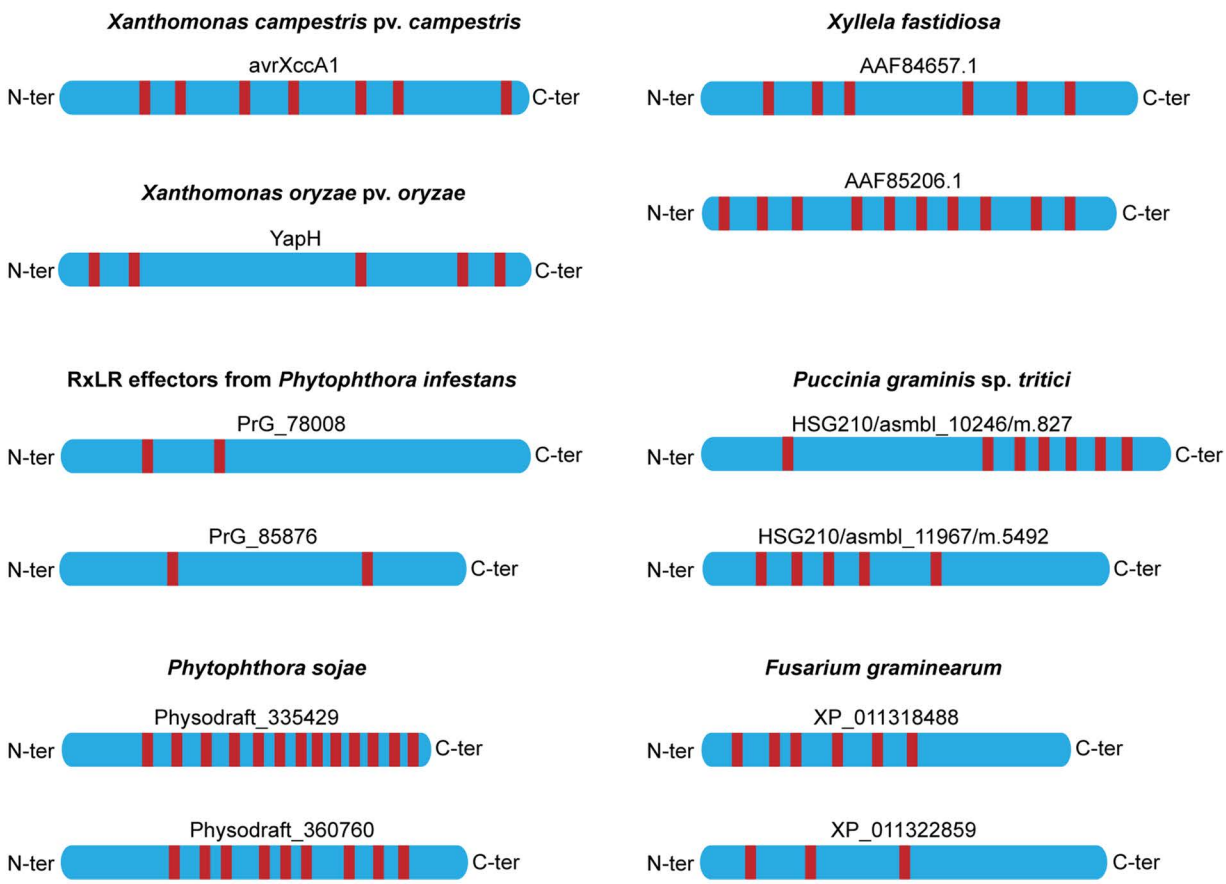

Supplemental Figure 6. Several effectors encoded by agriculturally important phytopathogens contain canonical GW/WG motifs
Effectors encoded by bacteria (*Xanthomonas campestris*, *Xanthomonas oryzae* and *Xyllela fastidiosa*), oomycetes (*Phytophthora infestans* and *Phytophthora sojae*) or fungi (*Puccinia graminis* and *Fusarium graminearum*) containing the highest score (matrix AGO-planVir) of GW/WG motifs prediction were retrieved by using the web portal http://www.comgen.pl/whub (Zielezinski A. & Karlowski WM, 2015). A red bar represents each GW or WG motif.